Effects of the virtual particle number on the S matrix of the $(\phi^4)_{1+1}$ model

H. Kröger, R. Girard, and G. Dufour
Département de Physique, Université Laval, Québec, P.Q., Canada G1K 7P4
(Received 19 September 1986; revised manuscript received 19 January 1987)

We present results of the S matrix in the $(\phi^4)_{1+1}$ model obtained by a nonperturbative calculation using a momentum-space discretization technique. First, we calculate the two-body S matrix in the strong-coupling regime (up to $\lambda_{\text{eff}}=3$), with the restriction of taking into account only two-body virtual particle states. We find agreement with standard perturbation theory obtained by summing up the corresponding graphs to infinite order. We also estimate the effect of mass renormalization. Second, we investigate the effect of including higher virtual particle numbers in two-particle scattering in the cases $\lambda_{\text{eff}}=\frac{1}{6}$ and $\lambda_{\text{eff}}=1$. In both cases we find convergence of the S matrix with respect to increasing the virtual-particle-number cutoff.

I. INTRODUCTION

One of the topics of current research in field theory are nonperturbative solution methods. For a review see Ref. 1. Much progress has been made on sum rules and coordinate-space lattice techniques. In this paper we want to draw attention to momentum-space discretization methods. This approach has been used by Brooks and Frautschi[2] to calculate ground and excited states in the Yukawa model and by Pauli[3] to compute ground and excited states of a many-nucleon system. The results of Ref. 2 for the Yukawa model have been improved by Pauli and Brodsky[4] by using Fourier-transformed light-cone variables.

The usefulness of momentum-space discretization for the computation of the S matrix has been proposed by Kröger.[5] Based on that method the S matrix has been calculated for the $(\phi^4)_{1+1}$ model[6] and the nonlinear Schrödinger model.[7] The nonlinear Schrödinger model is a nonrelativistic field theory, which conserves the particle number and has an analytically known S matrix. It has served the purpose to test the latter nonperturbative computation method in the weak- as well as in the strong-coupling regime. The method was found to give results converging to the correct answer in all cases. The $(\phi^4)_{1+1}$ model on the other hand is a relativistic field theory, which does not conserve the particle number. In Ref. 6 the method has been applied in the weak-coupling regime to calculate a two-body S matrix and agreement was found with first-order perturbation theory. These calculations were parametrized by the following systematic approximation parameters: a momentum-space cutoff Λ, a partition of the momentum-space interval $[-\Lambda,\Lambda]$ in ν cells, a virtual-particle-number cutoff n, and a scattering time parameter T.

In the present paper, we want to extend the analysis of Ref. 6 for the S matrix of the $(\phi^4)_{1+1}$ model. In principle, one would like to extend the calculations with respect to the approximation parameters Λ, ν, and n. Computer storage limitations, however, impose practical constraints. Thus we have chosen to extend the calculations of Ref. 6 in two directions. Firstly, we increase the momentum-space basis, but freeze the virtual-particle-number degree of freedom. Secondly, we increase the virtual particle number, but freeze the momentum-space degrees of freedom.

In the first part, we have performed calculations in the strong-coupling regime. As in the calculations of Ref. 6, we have considered two-particle scattering and kept the number of virtual particles at two. However, we have increased the discrete momentum-space basis. From general physical grounds and also from experience gained on the nonlinear Schrödinger model,[7] one expects that, going from a small- to large-coupling constant, one would have to increase the momentum cutoff, the number of momentum-space cells, and the particle number cutoff. So with respect to the virtual-particle-number cutoff, the results reported here are still preliminary. On the other hand, the results can be compared with standard perturbation theory. It corresponds to summing up to infinite order all Feynman diagrams with virtual two-particle states, which can be carried out analytically in $1+1$ dimensions. We have carried out calculations varying the effective coupling constant $\lambda_{\text{eff}}=\lambda/m^2$ in the range between 0 and 3, where λ and m denote the bare quartic coupling and the bare mass, respectively. In the small-coupling region $\lambda_{\text{eff}}\ll 1$, one obtains very good numerical agreement. In the strong-coupling region $\lambda_{\text{eff}}=1$ we find numerical agreement with an error on the order of 6%. Stevenson[8] has shown for the $(\phi^4)_{1+1}$ model, using the Gaussian-effective-potential method, that for $\lambda_{\text{eff}}=2.552$ the Gaussian effective potential evolves from a single well to a double well. Chang[9] found, using the Hartree approximation, that the Hartree effective potential goes from a single to a double well at $\lambda_{\text{eff}}=2.552$. He argues that it does not correspond to a first-order, but a second-order phase transition. Because of the indication that strong coupling only sets in at about $\lambda_{\text{eff}}=2.5$, we have also performed calculations for $\lambda_{\text{eff}}=3$. Again we find, for the S matrix, numerical agreement with an error on the order of 6%. The numerical results are discussed in Sec. II.

Another point which we want to address here is the

problem of renormalization. The $(\phi^4)_{1+1}$ model is superrenormalizable, i.e., one expects only finite counterterms in perturbative renormalization. The only irreducible divergent graph is the tadpole graph, which can be eliminated by normal ordering, which has been done in this work. In a nonperturbative renormalization procedure, one would have to determine a cutoff-dependent mass, coupling constant, etc., and fine-tune them accordingly such that observable quantities such as, e.g., cross sections, tend to a given limiting value when the cutoff Λ tends to infinity. We have calculated the renormalized mass m_R nonperturbatively by calculating the two-point Green's function including virtual three-particle states. It turns out that the renormalization gives negligible effects for m_R if the bare effective coupling constant λ_{eff} is small but has a non-negligible effect for $\lambda_{\text{eff}}=1$.

In the second part, we have performed calculations including higher virtual particle numbers. As mentioned above we have now restricted the momentum-space degrees of freedom. This has been done by choosing a basis of states corresponding to a given particle number and energy. The momentum-space degrees of freedom have been fixed by integrating over a given distribution. We have carried out calculations for $\lambda_{\text{eff}}=\frac{1}{6}$ and $\lambda_{\text{eff}}=1$. For $\lambda_{\text{eff}}=\frac{1}{6}$ we find, for the two-body elastic scattering S matrix, that virtual four-particle states give only a small contribution, and the contribution from virtual six-particle states is even more negligible. For $\lambda_{\text{eff}}=1$, however, one needs virtual twelve-particle states to give a contribution in the order of 1%. For example, in both cases one observes that the S matrix converges with respect to increasing the virtual-particle-number cutoff. The numerical results are discussed in Sec. III. Finally, Sec. IV gives some concluding remarks.

II. ELASTIC TWO-BODY S MATRIX IN THE STRONG-COUPLING REGIME

The aim of this section is to present an application of a nonperturbative time-dependent calculation scheme to the two-body scattering process in the $(\phi^4)_{1+1}$ model in the strong-coupling regime. The method has been discussed in Refs. 6 and 7, so we will recall only the basic aspects of the formalism. We consider the S matrix, given in the form

$$S=\text{w-}\lim_{t\to\infty}\exp(iH^0t)\exp(-2iHt)\exp(iH^0t)\ , \tag{2.1}$$

where H and H^0 denote the full and asymptotic Hamiltonian, respectively. In the following we will consider an S-matrix element $\langle\Omega_{\text{out}}\,|\,S\,|\,\Omega_{\text{in}}\rangle$, where Ω_{in}, Ω_{out} are asymptotically incoming and outgoing wave-packet states. We approximate the S matrix by

$$S_N(T)=\exp(iH_N^0T)\exp(-2iH_NT)\exp(iH_N^0T)\ , \tag{2.2}$$

where H_N and H_N^0 are finite-dimensional Hermitian approximations of H and H^0, respectively, and T is the time parameter. Note that $S_N(T)$ is unitary. The numerical calculation of $S_N(T)$ is performed using the eigenrepresentation of the finite-dimensional matrices H_N and H_N^0. H_N and H_N^0 are constructed via

$$H_N=P_NHP_N\ ,\quad H_N^0=P_NH^0P_N\ , \tag{2.3}$$

where P_N is an orthogonal projector on a finite-dimensional subspace of the Fock space. In this section we use the following finite-dimensional Fock space. We consider two-particle scattering and we also restrict the virtual particle number n to $n=2$. Let $[-\Lambda,\Lambda]$ denote a cutoff momentum-space interval and let $-\Lambda=k_0$, $k_1,\ldots,k_{\nu-1}$, $k_\nu=\Lambda$, $k_\mu<k_{\mu+1}$ denote a partition of the interval. Then we define creation operators, averaged over the cell μ, by

$$A_\mu^\dagger=\int dk\,\chi_\mu(k)A^\dagger(k)\Big/\int dk\,\chi_\mu(k)\ ,\quad \mu=1,2,\ldots,\nu\ , \tag{2.4}$$

where χ_μ is the characteristic function of cell μ. The finite-dimensional Fock space $\mathcal{F}_N$ is generated by

$$\mathcal{F}_{N=(\Lambda,\nu,n=2)}=\text{span of }\{A_\rho^\dagger A_\sigma^\dagger\,|\,0\rangle,\ \rho,\sigma=1,2,\ldots,\nu\}\ . \tag{2.5}$$

Because of symmetrization of the bosons, the basis can be restricted to states with $\rho\geq\sigma$. We denote the orthogonal basis states by

$$|\rho,\sigma\rangle=\kappa_{\rho\sigma}\,|\,A_\rho^\dagger A_\sigma^\dagger\rangle\ , \tag{2.6}$$

where $\kappa_{\rho\sigma}$ normalizes $|\rho,\sigma\rangle$ to unity.

The procedure to obtain the S matrix is to calculate $S_N(T)$ for a set of approximation parameters and then let the approximation parameters Λ, ν, n, T tend to infinity. The crucial question is the following: Does $S_N(T)$ converge and if so, to which limit? This has been studied numerically and will be discussed below. Because there are four approximation parameters and one does not expect uniform convergence, it is very useful for practical purposes to have some control of the error. One function, which serves that purpose, proposed in Ref. 10, is

$$\Delta_{<\ >}=\left|\frac{\langle\psi_{\text{out}}(N,T)\,|\,H\,|\,\psi_{\text{in}}(N,T)\rangle-\langle\Omega_{\text{out}}\,|\,H^0\,|\,\Omega_{\text{in}}\rangle}{\langle\Omega_{\text{out}}\,|\,H^0\,|\,\Omega_{\text{in}}\rangle}\right|, \tag{2.7}$$

where

$$|\,\psi_{\substack{\text{out}\\\text{in}}}(N,T)\rangle=\exp(-iH_NT)\exp(iH_N^0T)\,|\,\Omega_{\substack{\text{out}\\\text{in}}}\rangle\ . \tag{2.8}$$

For nonrelativistic p-p scattering, the function $\Delta_{<\ >}$ turned out to be useful.[10] It reflects the intertwining property of the wave operators with the full and asymptotic Hamiltonian. When N and T tend to infinity, $\Delta_{<\ >}$ should go to zero. Another function to control the error, proposed in Ref. 7, is

$$\Delta_0=\left|\frac{\langle\Omega_{\text{out}}\,|\,S_N(T)-(H^0)^{-1}S_N(T)H^0\,|\,\Omega_{\text{in}}\rangle}{\langle\Omega_{\text{out}}\,|\,S_N(T)\,|\,\Omega_{\text{in}}\rangle}\right|, \tag{2.9}$$

which should be applied to only those asymptotic wave-packet states on which H^0 is invertible. This function reflects the commutation property of the S matrix with the asymptotic Hamiltonian. It should go to zero, too, when N and T tend to infinity. Experience gained from models, where the exact S matrix is known, has shown

that a minimum in the error of the S matrix,

$$\Delta=\left|\frac{\langle\Omega_{\text{out}}|S-S_N(T)|\Omega_{\text{in}}\rangle}{\langle\Omega_{\text{out}}|S|\Omega_{\text{in}}\rangle}\right|, \tag{2.10}$$

coincides with a minimum in the function $\Delta_{<\ >}$ and Δ_0, respectively. Thus, for models where the exact S matrix is unknown, we will search for minima of $\Delta_{<\ >}$, Δ_0 in order to constraint the domain of approximation parameters.

Now let us consider, in particular, the $(\phi^4)_{1+1}$ model, given by the Hamiltonian

$$\begin{aligned} H&=H^0+H^{\text{int}}, \\ H^0&=:\tfrac{1}{2}\int dx\,\partial_\mu\phi\partial^\mu\phi+m^2\phi^2:, \\ H^{\text{int}}&=:\lambda\int dx\,\phi^4:. \end{aligned} \tag{2.11}$$

The field ϕ obeys the canonical commutation relations

$$[\phi(x,t),\phi(y,t)]=i\delta(x-y) \tag{2.12}$$

and admits the Fourier representation

$$\begin{aligned} \phi(x,t=0)&=\frac{1}{2\pi}\int\frac{dk}{2E^0(k)}[A(k)e^{ikx}+A^\dagger(k)e^{-ikx}], \\ E^0(k)&=(k^2+m^2)^{1/2}. \end{aligned} \tag{2.13}$$

Now we can express the matrix elements of the Hamiltonian in terms of the finite-dimensional basis, defined by Eq. (2.6) [note: the normalization of $A(k)$ is fixed by Eqs. (2.12) and (2.13)]. Denoting

$$E^0_\sigma=\langle\sigma|H^0|\sigma\rangle, \tag{2.14}$$

one can express the matrix elements of H^0 as

$$\langle\sigma,\rho|H^0|\tau,\omega\rangle=(E^0_\sigma+E^0_\rho)\delta_{\sigma,\tau}\delta_{\rho,\omega} \tag{2.15}$$

and matrix elements of H^{int} as

$$\langle\sigma,\rho|H^{\text{int}}|\tau,\omega\rangle=\frac{2\pi 4!\lambda\Delta k\,\delta_{\sigma+\rho,\tau+\omega}}{(b_\rho b_\sigma b_\tau b_\omega)^{1/2}}, \tag{2.16}$$

where Δk is the distance between two nodes in an equidistant partition of $[-\Lambda,+\Lambda]$ and

$$b_\sigma=2\pi E^0_\sigma. \tag{2.17}$$

One should notice that the matrix element in this basis conserves the discretized total momentum. Moreover, after splitting off the total momentum-conserving δ function, the matrix element is separable. This property facilitates the numerical solution of the diagonalization of H by reducing the algebraic dimension. We denote by α the conserved discretized total momentum. For each such α there is an invariant subspace. We solve the diagonalization problem independently in each invariant subspace

$$H_{N,\alpha}|\phi_{\alpha,\beta}\rangle=E_{\alpha,\beta}|\phi_{\alpha,\beta}\rangle. \tag{2.18}$$

According to Eq. (2.16), the interaction can be written in the subspace α

$$P_{N,\alpha}H^{\text{int}}P_{N,\alpha}=|\Xi_\alpha\rangle\lambda\langle\Xi_\alpha|, \tag{2.19}$$

where $|\Xi_\alpha\rangle$ is given by

$$\langle\sigma,\rho|\Xi_\alpha\rangle=\delta_{\alpha,\sigma+\rho}\left[\frac{2\pi 4!\Delta k}{b_\sigma b_\rho}\right]^{1/2}. \tag{2.20}$$

Equation (2.19) clearly exhibits the separability property. This property allows one to transform the eigenvalue equation (2.18) in two simpler equations: namely,

$$\lambda^{-1}=\sum_{\sigma,\rho}\frac{|\langle\sigma,\rho|\Xi_\alpha\rangle|^2}{E_{\alpha,\beta}-(E^0_\sigma+E^0_\rho)}, \tag{2.21}$$

which determines the eigenvalue $E_{\alpha,\beta}$, and

$$\langle\sigma,\rho|\phi_{\alpha,\beta}\rangle=\kappa_{\alpha,\beta}\frac{\langle\sigma,\rho|\Xi_\alpha\rangle}{E_{\alpha,\beta}-(E^0_\sigma+E^0_\rho)}, \tag{2.22}$$

which determines the eigenvector $\phi_{\alpha,\beta}$, $\kappa_{\alpha,\beta}$ being a normalization constant.

Finally we want to specify the asymptotic wave packets Ω_{in}, Ω_{out}. Let

$$|\Omega_i\rangle=\kappa_i\int_{k_{i\,\text{low}}}^{k_{i\,\text{up}}}dk\{1-\cos[2\pi(k-k_{i\,\text{low}})/(k_{i\,\text{up}}-k_{i\,\text{low}})]\}A^\dagger(k)|0\rangle \tag{2.23}$$

denote a one-particle asymptotic wave packet. It has the properties of being a bell-shaped distribution between $k_{i\,\text{low}}$ and $k_{i\,\text{up}}$, vanishing outside, having a maximum at $(k_{i\,\text{up}}+k_{i\,\text{low}})/2$, and having a half-width of $(k_{i\,\text{up}}-k_{i\,\text{low}})/2$. We take

$$|\Omega_{\text{in}}\rangle=|\Omega_{\text{out}}\rangle=|\Omega_1,\Omega_2\rangle, \tag{2.24}$$

where Ω_1, Ω_2 are distinguished by the parameters $k_{i\,\text{low}}, k_{i\,\text{up}}$. Now let us discuss the numerical results. The asymptotic wave packets are specified by $k_{1\,\text{low}}=0.25$ MeV, $k_{1\,\text{up}}=0.5$ MeV, $k_{2\,\text{low}}=0.75$ MeV, $k_{2\,\text{up}}=1.0$ MeV. In Table I we display the results for the model parameters $m=1.0$ MeV, $\lambda=10^{-2}$ MeV^2, i.e., $\lambda_{\text{eff}}=10^{-2}$, and the approximation parameters $\Lambda=4.0$ MeV, $n=2$.

We display the dependence of $S_N(T)$ on ν and T. The numerical result is stable within four digits at $\nu=500$, $T=600$ MeV^{-1}. In Fig. 1 we show for $\nu=500$ the dependence of $\text{Im}[S_N(T)]$ on the time parameter, together with the error criterion Δ_0, given by Eq. (2.9). Δ_0 exhibits a sharp minimum at $T=620$ MeV^{-1}. One notices that in the neighborhood of that time parameter the imaginary part of $S_N(T)$ (and also the real part, not displayed here) is very stable. In this case the coupling constant is small compared to the mass, i.e., we are in the small-coupling region. We have compared our nonperturbative result $S_N(T)$ with first-order standard perturbation theory, which gives $S^{(1)}=1.0-0.1391i$ which deviates from $S_N(T)$ in the real part on the order of 1.0×10^{-2}, and in

TABLE I. Dependence of the S-matrix element $\langle \Omega_{\text{out}} | S_N(T) | \Omega_{\text{in}} \rangle$ for two-body scattering on the number ν of expansion functions and the scattering time T. The model parameters are mass $m=1.0$ MeV, coupling constant $\lambda=0.01$ MeV^2; the approximation parameters are momentum cutoff $\Lambda=4.0$ MeV, and virtual-particle-number cutoff $n=2$.

T(MeV^{-1}) \ ν	300	400	500
0	(1.0000, 0.0000)	(1.0000, 0.0000)	(1.0000, 0.0000)
40	(0.9957, −0.0607)	(0.9957, −0.0607)	(0.9957, −0.0607)
80	(0.9925, −0.1057)	(0.9925, −0.1058)	(0.9925, −0.1058)
120	(0.9909, −0.1284)	(0.9909, −0.1284)	(0.9909, −0.1284)
160	(0.9903, −0.1368)	(0.9903, −0.1368)	(0.9903, −0.1368)
200	(0.9901, −0.1391)	(0.9901, −0.1391)	(0.9901, −0.1391)
240	(0.9901, −0.1397)	(0.9901, −0.1397)	(0.9901, −0.1396)
280	(0.9901, −0.1398)	(0.9901, −0.1398)	(0.9901, −0.1398)
320	(0.9900, −0.1399)	(0.9900, −0.1399)	(0.9900, −0.1399)
360	(0.9900, −0.1399)	(0.9900, −0.1399)	(0.9900, −0.1399)
400		(0.9900, −0.1399)	(0.9900, −0.1399)
440		(0.9900, −0.1399)	(0.9900, −0.1399)
480		(0.9900, −0.1399)	(0.9900, −0.1399)
520			(0.9900, −0.1399)
560			(0.9900, −0.1399)
600			(0.9900, −0.1399)

the imaginary part on the order of 0.8×10^{-3}.

In Table II we display the results for a strong-coupling case, where we took $\lambda=1.0$ MeV^2, i.e., $\lambda_{\text{eff}}=1$. Again we find numerical stability of $S_N(T)$ at $\nu=500$, $T=600$ MeV^{-1}. For this region of the coupling constant, first-order perturbation theory is certainly not valid. Because we have restricted in the calculation of $S_N(T)$ the virtual particle number to two, $S_N(T)$ should correspond to standard perturbation theory summing up all graphs with two virtual particles, as shown in Fig. 2. For the $(\phi^4)_{1+1}$ model these graphs can be summed to infinite order to give

$$\langle A^\dagger(k_1')A^\dagger(k_2') | S^{(\infty)} | A^\dagger(k_1)A^\dagger(k_2)\rangle = s\langle A^\dagger(k_1')A^\dagger(k_2') | A^\dagger(k_1)A^\dagger(k_2)\rangle ,$$

$$s=(1-\lambda X-iY)/(1-\lambda X+iY) ,$$

$$X=\frac{Y}{\pi}\ln|(1+4q^2Y)/(1-4q^2Y)| , \tag{2.25}$$

$$Y=\tfrac{1}{8}[k_1E^0(k_2)-k_2E^0(k_1)]^{-1} ,$$

$$q^2=(k_1+k_2)^2-[E^0(k_1)+E^0(k_2)]^2 .$$

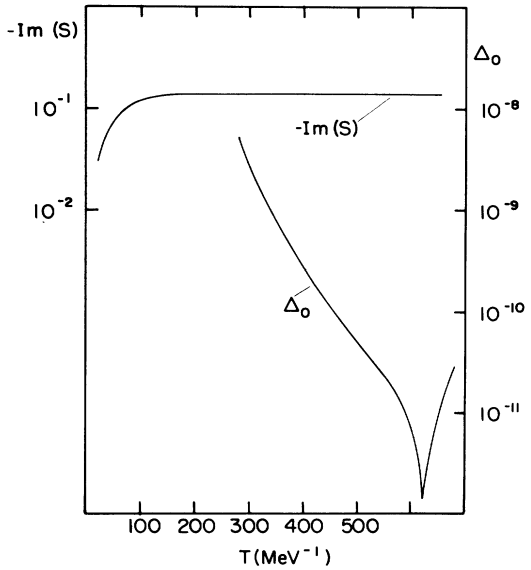

FIG. 1. Imaginary part of the S-matrix element $\langle \Omega_{\text{out}} | S_N(T) | \Omega_{\text{in}} \rangle$ as a function of the time T corresponding to the model parameters: coupling constant $\lambda=0.01$ MeV^2, mass $m=1.0$ MeV, and the approximation parameters: momentum cutoff $\Lambda=4.0$ MeV, number of expansion functions $\nu=500$, number of asymptotic and number of virtual particles $n=2$. The function Δ_0 displayed is a measure of the violation of energy conservation of the approximate S matrix $S_N(T)$. The minimum of Δ_0 coincides with a region of stability of $S_N(T)$.

Note that $S^{(\infty)}$ is unitary. In Table III we have compared the matrix element $\langle \Omega_{\text{out}} | S | \Omega_{\text{in}} \rangle$ calculated nonperturbatively, in first-order perturbation theory and in infinite order of perturbation theory. We have varied the coupling constant between $\lambda=0.01$ MeV^2 (small coupling) and $\lambda=3.0$ MeV^2 (strong coupling). In the nonperturbative calculation, we used the approximation parameters $\Lambda=4.0$ MeV, $\nu=300$, $n=2$. Note that due to the finite cutoff Λ, one violates Lorentz invariance. The results for $S_N(T)$, given in column two of Table III, each correspond to a T value, which gives a minimum of Δ_0. In the perturbation-theory calculations one has calculated the loop graph without imposing any momentum cutoff. One finds for $\lambda=0.01$ MeV^2 agreement between $S^{(1)}$, $S^{(\infty)}$, and $S_N(T)$ within 1%; however, for $\lambda=3.0$ MeV^2, $S^{(1)}$ differs by more than a factor of 40 from $S^{(\infty)}$. $S^{(\infty)}$ and $S_N(T)$ agree with an error in the order of 6%. We ascribe the latter deviation to the finiteness of the approximation parameters, in particular to the finite momentum-space cutoff Λ, used in $S_N(T)$.

TABLE II. Same as in Table I, but $\lambda = 1.0$ MeV^2.

T(MeV^{-1}) \ ν	300	400	500
300	(−0.9983, 0.04479)	(−0.9982, 0.04474)	(−0.9979, 0.04474)
320	(−0.9985, 0.04415)	(−0.9984, 0.04481)	(−0.9982, 0.04480)
340	(−0.9986, 0.04487)	(−0.9986, 0.04486)	(−0.9984, 0.04484)
360		(−0.9987, 0.04489)	(−0.9985, 0.04487)
380		(−0.9987, 0.04491)	(−0.9986, 0.04488)
400		(−0.9988, 0.04491)	(−0.9986, 0.04490)
420		(−0.9988, 0.04492)	(−0.9987, 0.04491)
440		(−0.9988, 0.04492)	(−0.9987, 0.04492)
460		(−0.9988, 0.04492)	(−0.9987, 0.04492)
480			(−0.9988, 0.04493)
500			(−0.9988, 0.04493)
520			(−0.9988, 0.04492)
540			(−0.9988, 0.04492)
560			(−0.9988, 0.04492)
580			(−0.9988, 0.04492)

So far we have discussed the results in terms of bare model parameters. The physical parameters, however, are not the bare ones, but the renormalized ones. We define the renormalized parameters, such as the mass m_R and the coupling constant λ_R, in the standard way via the two-point and four-point vertex Green's function, respectively.

The n-point Green's function, which is closely related to the time evolution and the S matrix, can be calculated in our nonperturbative scheme, i.e., in the approximation characterized by the parameters momentum cutoff Λ, the partition parameter ν, the virtual particle cutoff n, and the scattering time T. In this paper we have calculated the renormalized mass. The renormalized mass corresponds to a pole in the two-point Green's function at momentum $k=0$, or a zero in the inverse Green's function. Hence we have calculated the lowest eigenvalue of the Hamiltonian, corresponding to $k=0$, in the approximation of cutting off the virtual particular number by three. This is equivalent to sum up to infinite order all the bubbles of self-energy two-loop diagrams, i.e., the bubbles with three virtual particle states. The numerical results are given in Table IV. We have taken $m_{\text{bare}}=1$ MeV and varied $\lambda_{\text{eff,bare}}=\lambda_{\text{bare}}/m_{\text{bare}}{}^2$ between 0.01 and 2.0. We find for small coupling $\lambda_{\text{eff,bare}} \ll 1$ negligible effects on the renormalized mass m_R. However for strong coupling, $\lambda_{\text{eff,bare}}=1$, one observes a profound effect on m_R. There is a critical value $\lambda^{\text{crit}}_{\text{eff,bare}} \approx 1.5$, for which $m_R{}^2$ vanishes. For larger $\lambda_{\text{eff,bare}}$, $m_R{}^2$ becomes negative. This is not a contradiction to the observation from the Gaussian/Hartree effective-potential method,[8,9] where for large $\lambda_{\text{eff,bare}}$ a transition is found in the effective potential from a single well to a double well.

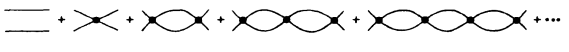

FIG. 2. Feynman graphs corresponding to asymptotic and virtual two-particle states.

III. EFFECTS OF HIGHER VIRTUAL PARTICLE NUMBERS

As mentioned in the Introduction we wanted to include states with higher numbers of virtual particles, which can be done at the cost of restricting the momentum-space degrees of freedom. In a first attempt we used a basis of states, where the states correspond to a good particle number, but momentum and energy degrees of freedom were averaged. We tried, in particular,

$$|j\rangle = \kappa_j \int dk_1 \cdots dk_j \chi(k_1,\ldots,k_j) \times A^\dagger(k_1)\cdots A^\dagger(k_j)|0\rangle ,$$
$$\chi(k_1,\ldots,k_j) = \begin{cases} 1 & \text{if } -\Lambda < k_1,\ldots,k_j < \Lambda , \\ 0 & \text{otherwise} , \end{cases} \tag{3.1}$$

where κ_j is a normalization constant. This attempt was unsuccessful, the S matrix did not converge. The reason can be understood from time-dependent nonrelativistic scattering theory. In the proof of existence of the wave operators, one has as an ingredient the property

$$\exp(iH^0 t) \underset{t\to\infty}{\overset{w}{\longrightarrow}} 0 . \tag{3.2}$$

A similar property has to hold for the time evolution of the finite-dimensional asymptotic Hamiltonian $\exp(iH_N^0 T)$. For each $\psi,\phi \in \mathscr{H}$, $\epsilon > 0$ exist N and $T \in \mathbf{R}$ such that

$$|\langle \psi | \exp(iH_N^0 T) | \phi \rangle < \epsilon , \tag{3.3}$$

i.e., for arbitrary Hilbert states ψ,ϕ the expression $\langle \psi | \exp(iH_N^0 T) | \phi \rangle$ can be made arbitrarily small. However, for the basis given in Eq. (3.1) this does not hold, which can be verified immediately: one observes that H_N^0 is diagonal in this basis. Then we take, e.g., $\psi = \phi = |1\rangle$.

TABLE III. Comparison of the S-matrix element $\langle \Omega_{\text{out}} | S | \Omega_{\text{in}} \rangle$ for two-body scattering calculated nonperturbatively $[S_N(T)]$ and in standard perturbation theory $(S^{(\infty)},S^{(1)})$ for different coupling constants. The model parameter is $m=1.0$ MeV. The approximation parameters used in the nonperturbative calculation are $\Lambda=4.0$ MeV, $\nu=300$, $n=2$. $S^{(\infty)}$ corresponds to summing to infinite order all graphs with virtual two-particle states; $S^{(1)}$ corresponds to first-order perturbation theory.

$\lambda(\text{MeV}^2)$	$S_N(T)$	$S^{(\infty)}$	$S^{(1)}$
0.01	(0.9900, −0.1399)	(0.9901, −0.1397)	(1.000, −0.1391)
0.02	(0.9599, −0.2788)	(0.9602, −0.2776)	(1.000, −0.2782)
0.03	(0.9100, −0.4122)	(0.9112, −0.4096)	(1.000, −0.4173)
0.04	(0.8422, −0.5360)	(0.8448, −0.5319)	(1.000, −0.5564)
0.05	(0.7592, −0.6470)	(0.7641, −0.6413)	(1.000, −0.6955)
0.06	(0.6645, −0.7429)	(0.6724, −0.7359)	(1.000, −0.8346)
0.07	(0.5617, −0.8224)	(0.5732, −0.8147)	(1.000, −0.9737)
0.08	(0.4546, −0.8855)	(0.4699, −0.8776)	(1.000, −1.113)
0.09	(0.3462, −0.9327)	(0.3655, −0.9254)	(1.000, −1.252)
0.10	(0.2393, −0.9652)	(0.2627, −0.9593)	(1.000, −1.391)
0.20	(−0.5227, −0.8474)	(−0.4802, −0.8721)	(1.000, −2.782)
0.30	(−0.8158, −0.5745)	(−0.7802, −0.6219)	(1.000, −4.173)
0.40	(−0.9251, −0.3766)	(−0.8995, −0.4344)	(1.000, −5.564)
0.50	(−0.9695, −0.2422)	(−0.9518, −0.3048)	(1.000, −6.955)
0.60	(−0.9885, −0.1481)	(−0.9768, −0.2129)	(1.000, −8.346)
0.70	(−0.9964, −0.0796)	(−0.9892, −0.1453)	(1.000, −9.737)
0.80	(−0.9993, −0.0277)	(−0.9955, −0.0940)	(1.000, −11.13)
0.90	(−0.9996, 0.0126)	(−0.9985, −0.0538)	(1.000, −12.52)
1.0	(−0.9986, 0.0449)	(−0.9998, −0.0215)	(1.000, −13.91)
3.0	(−0.9712, 0.2354)	(−0.9851, 0.1711)	(1.000, −41.73)

Hence

$$|\langle \psi | \exp(iH_N^0 T) | \phi \rangle| = |\langle 1 | 1 \rangle \exp(ih_{11}^0 T)| = 1 . \quad (3.4)$$

Hence in a second attempt, we have modified the basis in order to avoid this property. The minimal generalization from Eq. (3.1), is to take into account the energy degree of freedom, but still average over the momentum-space degrees of freedom. We took, in particular,

$$|\mu,j\rangle = \kappa_{\mu,j} \int dk_1 \cdots dk_j \int dE\, \chi(k_1,\ldots,k_j)\chi_\mu(E)\delta(E-[E^0(k_1)+\cdots+E^0(k_j)])A^\dagger(k_1)\cdots A^\dagger(k_j)|0\rangle , \quad (3.5)$$

$$\chi_\mu(E) = \begin{cases} 1 & \text{if } E_\mu < E < E_{\mu+1} , \\ 0 & \text{otherwise} , \end{cases}$$

where the function χ was taken as in Eq. (3.1) and $\kappa_{\mu j}$ normalizes the state to unity. This basis is orthogonal,

$$\langle \mu,i | \rho,j \rangle = \delta_{\mu\rho}\delta_{i,j} , \quad (3.6)$$

and H_N^0 is diagonal in the basis.

However, now the property (3.3) is valid because when $N \equiv (\Lambda,\nu,n)$ tends to infinity, the partition of the energy interval becomes finer and hence

$$\langle \psi | \exp(iH_N^0 T) | \phi \rangle = \sum_{\mu,j} \langle \psi | \mu,j \rangle \exp(ih_{\mu j}^0 T) \langle \mu j | \phi \rangle \underset{\Lambda,\nu\to\infty}{\to} \sum_j \int d\epsilon_j \langle \psi | \epsilon_j,j \rangle \exp(i\epsilon_j T) \langle \epsilon_j,j | \phi \rangle , \quad (3.7)$$

where $h_{\mu,j}^0 = \langle \mu,j | H_N^0 | \mu,j \rangle$ and $|\epsilon_j,j\rangle$ is a state of sharp asymptotic energy ϵ_j and particle number j. For each j the integral in the continuous variable ϵ_j tends to 0 when T tends to infinity, which is sufficient to guarantee the estimate (3.3).

Let us now fix the basis, given by Eq. (3.5), by specifying the finite-energy intervals and its partition. We have chosen the energy intervals in correlation with the particle number. To each particle number j we assign an interval

TABLE IV. The renormalized mass m_R as a function of the bare parameter $\lambda_{\text{eff,bare}} = \lambda_{\text{bare}}/m_{\text{bare}}^2$, where $m_{\text{bare}} = 1.0$ MeV. The sign in parentheses indicates that m_R^2 becomes negative.

$\lambda_{\text{eff,bare}}$	$m_{\text{ren}}(\text{MeV})$
0.01	0.999 954
0.1	0.995 486
1.0	0.593 981
2.0	(−)0.332 436

TABLE V. Dependence of the S-matrix element $\langle \Omega_{\text{out}} | S_N(T) | \Omega_{\text{in}} \rangle$ for two-body scattering, using the basis with increased virtual particle number given by Eq. (3.5), on the number ν of expansion functions and the scattering time T. The model parameters are $m=0.5$ MeV, $\lambda=\frac{1}{24}$ MeV^2, i.e., $\lambda_{\text{eff}}=\frac{1}{6}$. The approximation parameters are $\Lambda=1.0$ MeV, $n_{\min}=n_{\max}=n_{\text{in}}=n_{\text{out}}=2$.

T(MeV^{-1}) \ ν	10	20	30	40	50	70	90
10	0.9180	0.9063	0.9013	0.8988	0.8974	0.8957	0.8948
	$-0.3537i$	$-0.3796i$	$-0.3906i$	$-0.3956i$	$-0.3985i$	$-0.4020i$	$-0.4038i$
20	0.8552	0.8339	0.8248	0.8201	0.8176	0.8149	0.8136
	$-0.4773i$	$-0.5119i$	$-0.5262i$	$-0.5332i$	$-0.5367i$	$-0.5408i$	$-0.5429i$
30	0.8063	0.7794	0.7657	0.7582	0.7545	0.7507	0.7488
	$-0.5563i$	$-0.5939i$	$-0.6112i$	$-0.6203i$	$-0.6246i$	$-0.6294i$	$-0.6317i$
40		0.7373	0.7178	0.7073	0.7023	0.6967	0.6942
		$-0.6498i$	$-0.6705i$	$-0.6816i$	$-0.6868i$	$-0.6926i$	$-0.6952i$
50		0.6996	0.6781	0.6653	0.6585	0.6507	0.6472
		$-0.6939i$	$-0.7172i$	$-0.7263i$	$-0.7325i$	$-0.7396i$	$-0.7428i$
60		0.6597	0.6439	0.6288	0.6203	0.6093	0.6049
		$-0.7346i$	$-0.7482i$	$-0.7610i$	$-0.7679i$	$-0.7767i$	$-0.7802i$
70			0.6142	0.5966	0.5866	0.5724	0.5671
			$-0.7752i$	$-0.7887i$	$-0.7962i$	$-0.8063i$	$-0.8100i$
80			0.5687	0.5571	0.5397	0.5332	
			$-0.7996i$	$-0.8107i$	$-0.8187i$	$-0.8300i$	$-0.8341i$
90				0.5438	0.5315	0.5109	0.5032
				$-0.8288i$	$-0.8367i$	$-0.8490i$	$-0.8533i$
100				0.5198	0.5082	0.4863	0.4761
				$-0.8450i$	$-0.8520i$	$-0.8640i$	$-0.8693i$
110				0.4953	0.4871	0.4641	0.4521
				$-0.8600i$	$-0.8648i$	$-0.8766i$	$-0.8822i$
120					0.4680	0.4446	0.4313
					$-0.8757i$	$-0.8871i$	$-0.8927i$
130						0.4268	0.4118
						$-0.8960i$	$-0.9018i$
140						0.4103	0.3942
						$-0.9037i$	$-0.9094i$
150						0.3951	0.3780
						$-0.9105i$	$-0.9161i$
160						0.3812	0.3631
						$-0.9163i$	$-0.9218i$
170						0.3677	0.3500
						$-0.9215i$	$-0.9263i$
180						0.3542	0.3380
						$-0.9261i$	$-0.9301i$
190							0.3265
							$-0.9336i$
200							0.3147
							$-0.9370i$

$[E_j^{\text{low}}, E_j^{\text{up}}]$, with

$$E_j^{\text{low}} = jE^0(k=0) = jm \ , \qquad E_j^{\text{up}} = jE^0(k=\Lambda) = j(\Lambda^2+m^2)^{1/2} \ . \tag{3.8}$$

This choice corresponds for each momentum to the cutoff interval $[-\Lambda,\Lambda]$. Let $E_j^{\text{low}}=E_{0,j}$, $E_{1,j},\ldots,E_{\nu-1,j}$, $E_{\nu,j}=E_j^{\text{up}}$ denote an equidistant partition of the energy interval.

The numerical evaluation of the normalization $\kappa_{\mu j}$ of the states $|\mu,j\rangle$, the matrix elements $\langle \mu,j | H^0 | \mu,j \rangle$ and $\langle \mu,i | H^{\text{int}} | \rho,j \rangle$ involve high-dimensional integrals and has been carried out numerically using a Monte Carlo technique.[11] Although for high-dimensional integrals, the Monte Carlo technique is superior to fixed mesh-point integration methods, the evaluation of the matrix elements consumes the largest part of the computer time in the numerical calculation. Computer time can be saved by taking regard of symmetries or conservation rules. For example, $\langle \mu,i | H^{\text{int}} | \rho,j \rangle$ is a Hermitian matrix, so only half of the matrix elements have to be calculated. Because of the ϕ^4 interaction, the matrix element $\langle \mu,i | H^{\text{int}} | \rho,j \rangle$ gives nonzero contributions only for $i-j=0, \pm 2, \pm 4$, i.e., the interaction completely reduces the Fock space in an even-particle number sector and an odd-particle number sector. For the sake of simplicity, we have only considered the even-particle number sector.

We have taken the following asymptotic incoming and outgoing wave-packet states. All asymptotic wave packets are states corresponding to a pure asymptotic particle number. We took, corresponding to a given asymptotic particle number j, the following distribution:

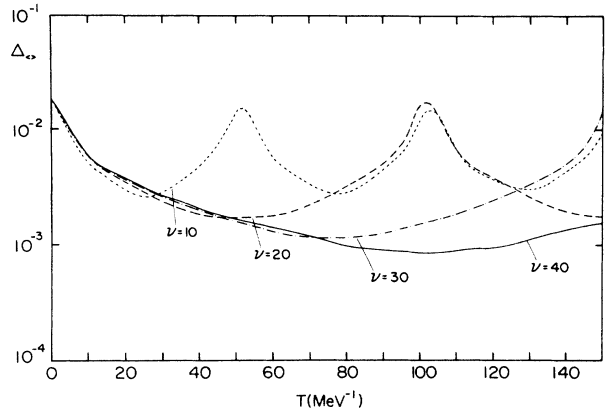

FIG. 3. Graph of the function $\Delta_{<\ >}$ measuring the violation of energy conservation of $S_N(T)$.

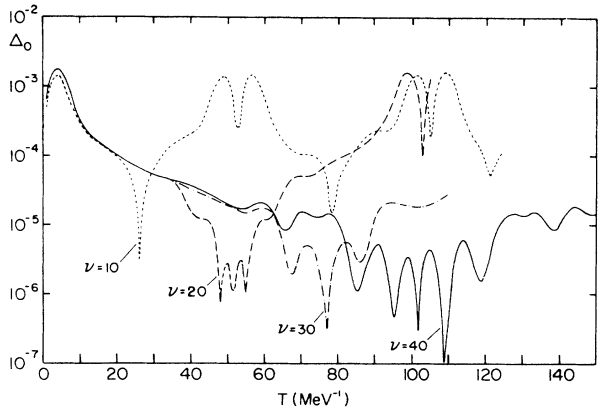

FIG. 4. Graph of the function Δ_0 measuring the violation of energy conservation of $S_N(T)$.

$$|\Omega,j\rangle=\kappa_j\sum_{\mu}\{1-\cos[2\pi(E_j^{\rm up}-E_{\mu,j})/(E_j^{\rm up}-E_j^{\rm low})]\}\,|\mu,j\rangle\ , \tag{3.9}$$

where κ_j normalizes the state to unity. We have taken this type of state as incoming as well as outgoing asymptotic state $\Omega_{\rm in}$, $\Omega_{\rm out}$.

The numerical results are displayed in Figs. 3 and 4 and Tables V–X. The model parameters chosen are $m=0.5$ MeV, $\lambda=\frac{1}{24}$ MeV^2, i.e., $\lambda_{\rm eff}=\frac{1}{6}$ and $\lambda=\frac{1}{4}$ MeV^2, i.e., $\lambda_{\rm eff}=1$. Tables V–VII and Figs. 3 and 4 correspond to $\lambda_{\rm eff}=\frac{1}{6}$, while Tables VIII–X correspond to $\lambda_{\rm eff}=1$. In all cases we have taken the momentum cutoff $\Lambda=1.0$ MeV. Table V displays the dependence of the matrix element $\langle\Omega_{\rm out}|S_N(T)|\Omega_{\rm in}\rangle$ on the number ν of expansion functions and the time parameter T. In this case we took $\Omega_{\rm out}$ and $\Omega_{\rm in}$ as two-particle states and considered only virtual two-particle states. If we denote by $n_{\rm in}$, $n_{\rm out}$ the

TABLE VI. Same as in Table V, but for four-body scattering, $n_{\rm min}=n_{\rm max}=n_{\rm in}=n_{\rm out}=4$.

T(MeV^{-1}) \ ν	10	20	30	40	50	70	90
10	−0.4777	−0.5183	−0.5278	−0.5312	−0.5343	−0.5378	−0.5396
	−0.3259i	−0.1987i	−0.1605i	−0.1352i	−0.1237i	−0.1098i	−0.1022i
20	−0.4502	−0.3945	−0.3381	−0.3087	−0.2973	−0.2803	−0.2727
	0.1090i	0.2096i	0.2552i	0.2785i	0.2884i	0.3016i	0.3070i
30		−0.2090	−0.1367	-0.8356×10^{-1}	-0.5483×10^{-1}	-0.2843×10^{-1}	-0.1578×10^{-1}
		0.3600i	0.3728i	0.3745i	0.3750i	0.3720i	0.3713i
40			0.3465×10^{-1}	0.8307×10^{-1}	0.1143	0.1507	0.1639
			0.4013i	0.3798i	0.3673i	0.3453i	0.3361i
50				0.2132	0.2365	0.2717	0.2859
				0.3465i	0.3203i	0.2837i	0.2622i
60					0.3311	0.3623	0.3737
					0.2559i	0.2060i	0.1771i
70						0.4236	0.4287
						0.1205i	$0.8441\times10^{-1}i$
80						0.4566	0.4573
						$0.3348\times10^{-1}i$	$-0.8920\times10^{-2}i$
90							0.4672
							−0.1001i
100							0.4675
							−0.1833i
110							0.4527
							−0.2587i
120							0.4357
							−0.3334i

TABLE VII. Dependence of the S-matrix element $\langle \Omega_{\text{out}} | S_N(T) | \Omega_{\text{in}} \rangle$ for two-particle scattering on the number ν of expansion functions and on the virtual-particle-number cutoff, i.e., $n_{\text{in}}=n_{\text{out}}=2$. The scattering time T has been chosen in all cases to correspond to a minimum of the function $\Delta_{<\ >}$.

$n_{\min}$ $n_{\max}$ \ ν	10	20	30	40	50	70	90
2 2	0.8263	0.6801	0.5966	0.5150	0.4757	0.3568	0.3392
	$-0.5261i$	$-0.7145i$	-0.7900	$-0.8481i$	$-0.8714i$	$-0.9253i$	$-0.9197i$
2 4	0.8727	0.7444	0.6686	0.5928	0.5561		
	$-0.4615i$	$-0.6555i$	$-0.7353i$	$-0.7977i$	$-0.8234i$		
2 6	0.8744	0.7467	0.6712	0.5957			
	$-0.4590i$	$-0.6531i$	$-0.7330i$	$-0.7956i$			
2 8	0.8745	0.7469	0.6686	0.5959			
	$-0.4589i$	$-0.6530i$	$-0.7355i$	$-0.7955i$			

TABLE VIII. Same as in Table V, but $\lambda=\frac{1}{4}$ MeV^2, i.e., $\lambda_{\text{eff}}=1$.

T(MeV^{-1}) \ ν	10	20	30	40	50	70	90
10	-0.5350	-0.5498	-0.5471	-0.5453	-0.5461	-0.5468	-0.5476
	$0.1648i$	$0.2539i$	$0.2879i$	$0.3065i$	$0.3162i$	$0.3274i$	$0.3333i$
20	-0.6070	0.6565×10^{-2}	0.4109×10^{-1}	0.5980×10^{-1}	0.6813×10^{-1}	0.7588×10^{-1}	0.7961×10^{-1}
	$0.4445i$	$0.5129i$	$0.5333i$	$0.5404i$	$0.5441i$	$0.5518i$	$0.5559i$
30		0.2935	0.3463	0.3727	0.3817	0.3926	0.3981
		$0.4066i$	$0.3976i$	$0.3879i$	$0.3840i$	$0.3836i$	$0.3841i$
40		0.4155	0.4785	0.5019	0.5091	0.5179	0.5230
		$0.2867i$	$0.2325i$	$0.2066i$	$0.1967i$	$0.1964i$	$0.1837i$
50		0.4777	0.5311	0.5437	0.5458	0.5495	0.5524
		$0.1693i$	$0.8660\times10^{-1}i$	$0.5053\times10^{-1}i$	$0.3284\times10^{-1}i$	$0.1388\times10^{-1}i$	$0.6552\times10^{-2}i$
60			0.5469	0.5389	0.5315	0.5244	0.5247
			$-0.3963\times10^{-1}i$	$-0.8431\times10^{-1}i$	$0.1014i$	$-0.1355i$	$-0.1440i$
70			0.5347	0.5042	0.4842	0.4630	0.4585
			$-0.1488i$	$-0.1996i$	$-0.2192i$	$-0.2533i$	$-0.3613i$
80				0.4523	0.4218	0.3836	0.3722
				$-0.2897i$	$-0.3040i$	$-0.3384i$	$-0.3426i$
90				0.3954	0.3568	0.3025	0.2840
				$-0.3576i$	$-0.3647i$	$-0.3943i$	$-0.3936i$
100				0.3320	0.2916	0.2315	0.2033
				$-0.4112i$	$-0.4090i$	$-0.4254i$	$-0.4202i$
110					0.2275	0.1624	0.1300
					$-0.4417i$	$-0.4455i$	$-0.4296i$
120						0.1022	0.6644×10^{-1}
						$-0.4533i$	$-0.4236i$
130						0.4824×10^{-1}	0.1584×10^{-1}
						$-0.4551i$	$-0.4107i$
140						-0.2102×10^{-2}	-0.3078×10^{-1}
						$-0.4487i$	$-0.3922i$
150						-0.4839×10^{-1}	-0.6795×10^{-1}
						$-0.4379i$	$-0.3729i$
160						-0.8391×10^{-1}	-0.9548×10^{-1}
						$-0.4256i$	$-0.3532i$
170						-0.1201	-0.1157
						$-0.4061i$	$-0.3233i$
180							-0.1282
							$-0.2930i$
190							-0.1351
							$-0.2660i$

TABLE IX. Same as in Table VI, but $\lambda=\frac{1}{4}$ MeV^2, i.e., $\lambda_{\text{eff}}=1$.

T(MeV^{-1}) \ ν	10	20	30	40	50	70	90
10	0.8500×10^{-1}	0.9580×10^{-1}	0.1037	-0.6398×10^{-1}	-0.8095×10^{-1}	−0.1075	−0.1123
	$0.4995i$	$-0.2004i$	$-0.2481i$	$-0.2122i$	$-0.2075i$	$-0.2029i$	$-0.2035i$
20		−0.2609	0.1504	−0.1767	−0.2453	−0.2890	−0.3120
		$-0.1687i$	$-0.3645i$	$-0.3103i$	$-0.2501i$	$-0.1733i$	$-0.1213i$
30			-0.9626×10^{-1}	0.3189	−0.3916	0.3543	0.2945
			$0.4290i$	$0.2497i$	$0.8910\times10^{-1}i$	$-0.1077i$	$-0.1783i$
40				-0.4435×10^{-1}	−0.3089	−0.4180	−0.3742
				$-0.4982i$	$-0.3511i$	$-0.6127\times10^{-1}i$	$0.7502\times10^{-1}i$
50					−0.2580	0.1263	0.2601
					$0.4358i$	$0.4623i$	$0.3270i$
60						0.5218	0.3412
						$-0.1568i$	$-0.3167i$
70						-0.5029×10^{-1}	−0.3099
						$-0.5931i$	$-0.4336i$
80							−0.5234
							$0.1794i$
90							-0.7315×10^{-1}
							$0.5505i$
100							0.3758
							$0.3649i$

asymptotic incoming and outgoing particle numbers, respectively, and by $n_{\min}$, $n_{\max}$ a lower and an upper cutoff in the virtual particle number, then we have in this case $n_{\text{in}}=n_{\text{out}}=n_{\min}=n_{\max}=2$. In Table VI we have presented the analogous results for $n_{\text{in}}=n_{\text{out}}=n_{\min}=n_{\max}=4$. One observes a noticeable but slow convergence in ν and T in all cases which is even slower as the particle number becomes higher. In Fig. 3 we display the function $\Delta_{<\ >}$, which is a measure of the violation of energy conservation of $S_N(T)$. One observes that with increased number ν of expansion functions the minimum of $\Delta_{<\ >}$ becomes deeper and broader. Also, one observes a quasiperiodic structure of $\Delta_{<\ >}$, while the relevant minimum is the first one. Experience with cases (see Ref. 10) where the exact S matrix is known shows that the minimum region of $\Delta_{<\ >}$ corresponds to a minimum in the error of $S_N(T)$ and a region of stability of $S_N(T)$. Hence, guided by that experience, we take $T=T_{\min}$ corresponding to a minimum in $\Delta_{<\ >}$ as the optimal value in $S_N(T)$. In analogy to Fig. 3, in Fig. 4 the graph of the function Δ_0 is displayed, which serves the same purpose. While in the results of Sec. II, with many momentum-space expansion functions, it turned out that Δ_0 is a suitable function, Fig. 4 shows in our present case a less appealing structure: namely, no clear unique minimum. However, the region where several minima occur close together corresponds to the region in Fig. 3 where $\Delta_{<\ >}$ has a minimum. Finally in Table VII we display the effect of including states of virtual particle number off the asymptotic particle number. We display $\langle\Omega_{\text{out}}|S_N(T)|\Omega_{\text{in}}\rangle$, with $T=T_{\min}$ corresponding to $\Delta_{<\ >}$, as a function of the number ν of expansion func-

TABLE X. Same as in Table VII, but $\lambda=\frac{1}{4}$ MeV^2, i.e., $\lambda_{\text{eff}}=1$.

$n_{\min}$ $n_{\max}$ \ ν	10	20	30	40	50	70	90
2 2	0.1016	0.4933	0.5152	0.3181	0.1907	−0.1455	−0.1351
	$0.4008i$	$0.1014i$	$-0.2083i$	$-0.4199i$	$-0.4540i$	−0.3821	$-0.2660i$
2 4	−0.5054	−0.8075	−0.4372	-0.1587×10^{-1}	0.1492		
	$-0.6862i$	$0.3622i$	$0.7575i$	$0.7695i$	$0.7004i$		
2 6	−0.1539	−0.8723	−0.7147	−0.3846			
	$-0.9384i$	$-0.1322i$	$0.3368i$	$0.4716i$			
2 8	0.3753×10^{-1}	−0.7771	−0.7100	−0.4361			
	$-0.9672i$	$-0.3320i$	$0.1198i$	$0.2768i$			
2 10	0.1188	−0.6757	−0.6535	−0.4241			
	$-0.9568i$	$-0.4395i$	$-0.1031\times10^{-2}i$	$0.1351i$			
2 12	0.1275	−0.6718	−0.6514	−0.4231			
	$-0.9562i$	$-0.4426i$	$-0.5187\times10^{-2}i$	$0.1308i$			

tions and the lower and upper cutoff in the virtual particle number. Table VII corresponds to $n_{\text{in}}=n_{\text{out}}=2$ (which has been reported in Table V for $n_{\min}=n_{\max}=2$). One observes convergence of the S matrix with respect to increasing the virtual-particle-number cutoff. Increasing the particle-number cutoff from 4 to 6 gives a contribution of 1%. In Tables VIII–X we display the corresponding results in the strong-coupling region $\lambda_{\text{eff}}=1$. In general one observes a convergence as in Tables V–VII, however, at a much slower rate. The most important results, in our opinion, are shown in Table X, demonstrating for $\lambda_{\text{eff}}=1$ convergence of the S matrix with respect to increasing the virtual-particle-number cutoff. However, a 1% contribution is only achieved if one increases the virtual-particle-number cutoff from 10 to 12.

IV. CONCLUSION

In this paper we have presented results of nonperturbative calculations of the S matrix of the $(\phi^4)_{1+1}$ model. The parameters which govern the systematic approximation scheme are a momentum-space cutoff Λ, a number ν of expansion functions, and a virtual-particle-number cutoff n and a scattering time T. In this work we have extended the results obtained earlier in the small-coupling regime[6] to the strong-coupling regime. We find also in the strong-coupling regime converged results. Because of computer storage limitations we have imposed the constraint of maximally two virtual particles for a two-particle scattering process, which is not physical in the strong-coupling regime. However, in this case it allows one to compare the nonperturbative result with standard perturbation theory, summing up to infinite order all graphs with two virtual particles, which can be done analytically. Agreement is found within numerical errors in the whole range of λ_{eff} up to $\lambda_{\text{eff}}=3$. In the case of a small coupling, agreement is also found with first-order perturbation theory. In order to test the sensitivity of the S matrix on higher virtual-particle-number states, we have used in Sec. III a basis of expansion functions, which takes into account the particle number and a discretization of energy, but averages over the momentum degrees of freedom. Using this basis we also find converged results with respect to the number of expansion functions and the time parameter. The calculations show that the S matrix $S_N(T)$ converges also with respect to increasing the upper cutoff in the virtual particle number. This is found for $\lambda_{\text{eff}}=\frac{1}{6}$, but most importantly, also for $\lambda_{\text{eff}}=1$.

ACKNOWLEDGMENTS

R.G. has been supported by la Formation de Chercheurs et l'Aide à la Recherche (FCAR); H.K. has been supported by the Natural Sciences and Engineering Research Council of Canada (NSERC). The authors are grateful to NSERC and Environment Canada for computer time on the CRAY 1-S.

[1]*Non-perturbative Methods,* workshop on Non-perturbative Methods, Montpellier, France, 1985, edited by S. Narison (World Scientific, Singapore, 1986).

[2]E. D. Brooks and S. C. Frautschi, Z. Phys. C **23**, 263 (1984).

[3]H. C. Pauli, Z. Phys. A **319**, 303 (1984).

[4]H. C. Pauli and S. J. Brodsky, Phys. Rev. D **32**, 1993 (1985); **32**, 2001 (1985).

[5]H. Kröger, J. Math. Phys. **24**, 1509 (1983); **25**, 1875 (1984).

[6]H. Kröger, A. Smailagic, and R. Girard, Phys. Rev. D **32**, 3221 (1985); R. Girard and H. Kröger, Phys. Lett. **164B**, 117 (1985); H. Kröger, A. Smailagic and R. Girard, Can. J. Phys. **64**, 611 (1986).

[7]R. Girard and H. Kröger, Phys. Rev. D **34**, 1824 (1986); Z. Phys. C **32**, 89 (1986).

[8]P. M. Stevenson, Phys. Rev. D **32**, 1389 (1985).

[9]S. J. Chang, Phys. Rev. D **13**, 2778 (1976); **12**, 1071 (1975).

[10]M. Batinić, Ž. Bajzer, and H. Kröger, Phys. Rev. C **33**, 1187 (1986).

[11]J. M. Hammersley and D. C. Handscomb, *Monte Carlo Methods* (Methuen, London, 1964).